University of Reading

Spontaneous local symmetry breaking: a conformational study of glycine on Cu{311}

Article

Accepted Version

Madden, D.C., Temprano, I., Sacchi, M. and Jenkins, S.J. (2015) Spontaneous local symmetry breaking: a conformational study of glycine on Cu{311}. Journal of Physical Chemistry C, 119 (23). pp. 13041-13049. ISSN 1932-7447 doi: https://doi.org/10.1021/acs.jpcc.5b02349 Available at https://centaur.reading.ac.uk/40249/

It is advisable to refer to the publisher's version if you intend to cite from the work. See Guidance on citing.

To link to this article DOI: http://dx.doi.org/10.1021/acs.jpcc.5b02349

Publisher: American Chemical Society

All outputs in CentAUR are protected by Intellectual Property Rights law, including copyright law. Copyright and IPR is retained by the creators or other copyright holders. Terms and conditions for use of this material are defined in the End User Agreement.

www.reading.ac.uk/centaur

CentAUR

University of Reading

Central Archive at the University of Reading

Reading's research outputs online

THE JOURNAL OF PHYSICAL CHEMISTRY C

Subscriber access provided by READING UNIV

Article

Spontaneous Local Symmetry Breaking: A Conformational Study of Glycine on Cu{311}

David C Madden, Israel Temprano, Marco Sacchi, and Stephen J. Jenkins

J. Phys. Chem. C, **Just Accepted Manuscript** • DOI: 10.1021/acs.jpcc.5b02349 • Publication Date (Web): 07 May 2015

Downloaded from http://pubs.acs.org on May 13, 2015

Just Accepted

"Just Accepted" manuscripts have been peer-reviewed and accepted for publication. They are posted online prior to technical editing, formatting for publication and author proofing. The American Chemical Society provides "Just Accepted" as a free service to the research community to expedite the dissemination of scientific material as soon as possible after acceptance. "Just Accepted" manuscripts appear in full in PDF format accompanied by an HTML abstract. "Just Accepted" manuscripts have been fully peer reviewed, but should not be considered the official version of record. They are accessible to all readers and citable by the Digital Object Identifier (DOI®). "Just Accepted" is an optional service offered to authors. Therefore, the "Just Accepted" Web site may not include all articles that will be published in the journal. After a manuscript is technically edited and formatted, it will be removed from the "Just Accepted" Web site and published as an ASAP article. Note that technical editing may introduce minor changes to the manuscript text and/or graphics which could affect content, and all legal disclaimers and ethical guidelines that apply to the journal pertain. ACS cannot be held responsible for errors or consequences arising from the use of information contained in these "Just Accepted" manuscripts.

ACS Publications
High quality. High impact.

The Journal of Physical Chemistry C is published by the American Chemical Society. 1155 Sixteenth Street N.W., Washington, DC 20036

Published by American Chemical Society. Copyright © American Chemical Society. However, no copyright claim is made to original U.S. Government works, or works produced by employees of any Commonwealth realm Crown government in the course of their duties.

Spontaneous Local Symmetry Breaking: A Conformational Study of Glycine on Cu{311}

David C. Madden, [†] Israel Temprano, Marco Sacchi, [‡] and Stephen J. Jenkins [*]

Department of Chemistry, University of Cambridge, Lensfield Road, Cambridge, CB2 1EW, UK

E-mail: sjj24@cam.ac.uk

[*]To whom correspondence should be addressed
[†]Department of Chemistry, University of Cambridge, Lensfield Road, Cambridge, CB2 1EW, UK
[‡]Department of Chemistry, University of Reading, Whiteknights, Reading, RG6 6AD

Abstract

Understanding the interplay between intrinsic molecular chirality and chirality of the bonding footprint is crucial in exploiting enantioselectivity at surfaces. As such, achiral glycine and chiral alanine are the most obvious candidates if one is to study this interplay on different surfaces. Here, we have investigated the adsorption of glycine on Cu{311} using reflection-absorption infrared spectroscopy, low-energy electron diffraction, temperature-programmed desorption and first-principles density-functional theory. This combination of techniques has allowed us to accurately identify the molecular conformations present under different conditions, and discuss the overlayer structure in the context of the possible bonding footprints. We have observed coverage-dependent local symmetry breaking, with three-point bonded glycinate moieties forming an achiral arrangement at low coverages, and chirality developing with the presence of two-point bonded moieties at high coverages. Comparison with previous work on the self-assembly of simple amino acids on Cu{311} and the structurally-similar Cu{110} surface has allowed us to rationalise the different conditions necessary for the formation of ordered chiral overlayers.

Keywords: Surface chirality, Amino acid, Self-organisation, RAIRS, LEED, DFT.

Introduction

The study of chirality at metal single-crystal surfaces has relevance to a broad range of applications including biocompatibility, bio-sensors and enantioselective heterogeneous catalysis.[1] Work is not limited to the behaviour of adsorbed chiral molecules on high-symmetry surfaces, and ranges from the chiral self-organisation of simple achiral molecules on achiral surfaces, to the enantiospecific restructuring of intrinsically chiral surfaces induced by chiral adsorbates.[1,2] With their low reactivity, copper surfaces provide ideal substrates on which to study the propagation of chirality from the molecular level to the mesoscopic level, and the formation of long-range chiral networks. In recent years, the behaviour of several simple amino acids on the low-index Cu{100} and Cu{110} surfaces has been studied extensively.[3–21] These include the simplest chiral amino acid, alanine ($H_2NCH(CH_3)COOH$), and glycine (H_2NCH_2COOH), which is unique amongst protein-forming α-amino acids because it is achiral.

Recently, the strong structural relationship between face-centred cubic (fcc) Cu{110} and Cu{311} surfaces has been recognised,[22,23] and the potential for comparison between the behaviour of amino acids on these two surfaces has begun to be exploited.[2,24,25] As can be seen in Figure 1, the unreconstructed Cu{110} and Cu{311} surfaces both have linear chains of close-packed top-layer atoms separated by steps, although the spacing of the close-packed rows is greater for Cu{311} (4.23 Å as opposed to 3.61 Å). In addition to the larger surface unit cell, the registry of adjacent close-packed rows differs on the two surfaces, with a primitive rectangular surface unit cell existing for Cu{110}, but not for Cu{311}.

This difference alters the possible bonding footprints (defined according to the surface atoms to which the molecule bonds)[2] that can be adopted by adsorbing α-amino acids; comparison of the bonding configurations adopted and the ordered overlayers formed on the two surfaces will, therefore, provide insight into the effect of small changes in surface structure and symmetry on the behaviour of adsorbed species. We have previously explored the self-assembly of

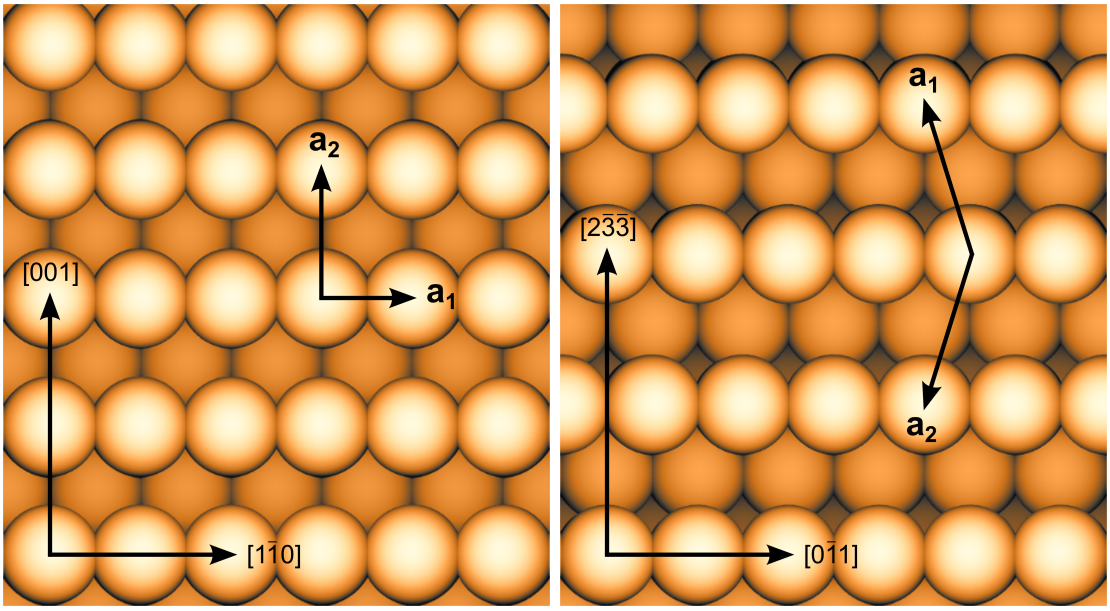

Figure 1: Schematic diagrams of the unreconstructed Cu(110) (left) and Cu(311) (right) surfaces. Key crystallographic directions are indicated on both surfaces, as are basis vectors, $\mathbf{a}_1$ and $\mathbf{a}_2$, defining primitive surface unit cells.

alanine on Cu{311},[24] and compared its behaviour to that reported on Cu{110}[3,13,15–19]. A significant difference relates to the formation of ordered phases on the two surfaces: whereas an ordered structure readily forms at 300 K on Cu{311}, ordered structures are only seen on Cu{110} after high-temperature annealing, emphasizing the effect that different bonding footprints can have on molecular self-assembly.

Here we report an experimental and computational investigation of the behaviour of glycine on Cu{311}. Although glycine is structurally similar to alanine, the absence of molecular chirality makes comparison of its behaviour on Cu{110} and Cu{311} insightful, as it allows us to focus on the impact of the bonding footprint. Using temperature-programmed desorption (TPD), low-energy electron diffraction (LEED), reflection-absorption infrared spectroscopy (RAIRS) and first-principles density functional theory (DFT) we have elucidated the preparation conditions leading to different phases, and the bonding configurations adopted by the adsorbed species within them. This has allowed us to compare the behaviour of glycine and alanine on Cu{311}, and rationalise the similarities and differences to the behaviour of the

same adsorbates on Cu{110} by considering the different surface structures in the two cases.

Experimental and Calculation Details

The experiments were performed in an ultra-high vacuum (UHV) chamber with base pressure around of 1×10^{-10} mbar, using a Cu crystal with dimensions of $15 \times 10 \times 1$ mm, cut to within 0.1° of the {311} plane and polished to a roughness of less than 0.03 μm. The surface was prepared with cycles of argon ion sputtering and annealing at 850 K, until a sharp (1×1) LEED pattern was observed. Unless otherwise stated, during experiments the Cu{311} surface temperature was 300 K. Glycine was dosed by resistively heating a capillary tube filled with glycine to around 340 K. Exposure values (in langmuir; 1 L = 10^{-6} Torr s = 1.33×10^{-6} mbar s) were calculated from the pressure rise in the chamber (monitored with a hot-filament ionisation gauge); a dosing pressure of 3×10^{-9} mbar was used unless otherwise stated. TPD data were obtained using a quadrupole mass spectrometer to monitor the partial pressures of the most significant fragments in the cracking pattern, whilst increasing the temperature of the crystal at a rate of 0.5 Ks^{-1}. LEED patterns were obtained at a very low incident beam energy, 19 eV, in order to prevent electron beam damage, to which amino acid overlayers are sensitive. RAIR spectra were obtained as the sum of 400 scans, at a resolution of 4 cm^{-1}, using a Mattson RS2 Fourier transform infrared (FTIR) spectrometer and external mercury cadmium telluride (MCT) detector; each sample spectrum was ratioed against a background obtained from the clean surface prior to dosing glycine. Where the effect of higher temperatures on the RAIR spectrum or LEED pattern was being studied, the crystal was annealed for two minutes at a higher temperature, then cooled back to 300 K before obtaining the data.

DFT calculations were performed using the CASTEP code,[26,27] at the generalised gradient approximation level of theory with the Perdew Burke Ernzerhof exchange-correlation functional.[28] The plane wave basis set was expanded to a 360 eV energy cut-off and recip-

rocal space was sampled with a $(3 \times 3 \times 1)$ Monkhorst–Pack k-point grid.[29] Electron-ion interactions were included within the ultrasoft pseudopotential scheme,[30] and van der Waals interactions were accounted for with the dispersion force correction methodology developed by Tkatchenko and Scheffler.[31] The force tolerance for the structural calculations was set to 0.04 eVÅ^{-1}, while the electronic energy was minimized up to a tolerance of 10^{-7} eV. Phonon spectra were calculated via the finite displacement method,[32] as we have described previously.[24] Our calculations assume in-phase motion between one unit cell and the next (i.e. we calculate only the zone-centre phonon modes), but this is entirely appropriate for comparison with RAIRS experiments. Calculated frequencies were multiplied by scaling factors of 0.99 (below 1800 cm^{-1}) and 0.96 (above 1800 cm^{-1}) to incorporate the effects of anharmonicity.[33] Assignment of particular displacement patterns to local-mode descriptions (e.g. carboxylate symmetric stretching, amine scissoring etc) was achieved by visual inspection.

Results and Discussion

Figure 2 shows TPD data obtained after dosing 6 L glycine at a Cu{311} surface temperature of 100 K. Two peaks are present, at around 320 and 500 K. Cracking of the parent ion in the mass spectrometer means that it has never been observed at significant levels in this system; however, comparison of the relative peak areas of different fragments at the two temperatures (and whilst dosing glycine) indicates the nature of the desorbing species. The ratio of the peak areas of the different fragments at 320 K is very similar to that observed whilst dosing; this suggests that the desorbing species leave the surface in a similar form to that in which they arrived, and so the peak corresponds to desorption of the physisorbed glycine multilayer. Relative to the peak area of the m/z = 44 (CO_2^+) fragment, that of m/z = 2 (H_2^+) is reproducibly six times larger at 500 K than at 320 K; likewise, the relative area of the m/z = 30 (H_4CN^+) peak decreases to one twentieth of the size at 500 K, compared to at 320 K. These changes suggest that dissociation of the chemisorbed monolayer occurs

prior to desorption. TPD data obtained after dosing glycine at 300 K (Figure S-1 of the Supporting Information) show no peak at 320 K, indicating that only a monolayer forms at this dosing temperature.

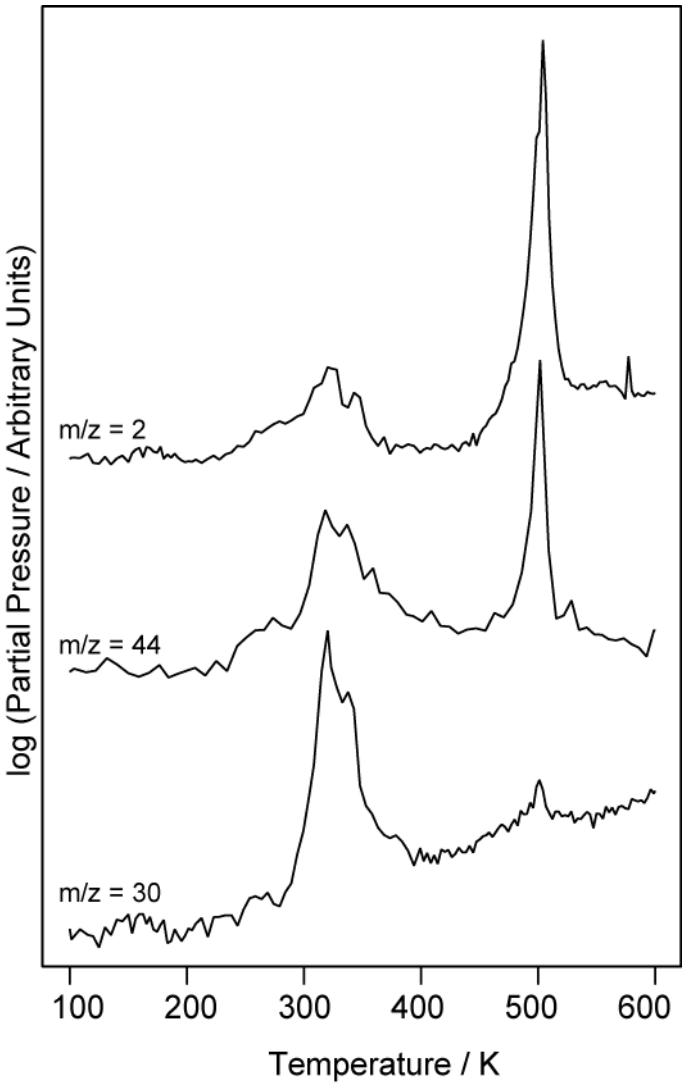

Figure 2: TPD data obtained at 0.5 Ks^{-1} after dosing 6 L glycine at 3×10^{-9} mbar and 100 K.

Figure 3 shows the development of the RAIR spectrum with increasing exposures of glycine at 300 K. Amino acids can exist in neutral, anionic, cationic and zwitterionic forms, depending on the protonation of the amine and carboxylic acid groups. The absence of a significant absorption due to the carbonyl stretch in neutral species, reported at 1723 cm^{-1} in multilayer spectra after dosing glycine onto Cu{110} at 85 K,[4] and observed at 1716 cm^{-1} in spectra

obtained on Cu{311} at 100 K (Figure S-2 of the Supporting Information), indicates that the carboxylic acid group of glycine deprotonates on adsorption at 300 K.

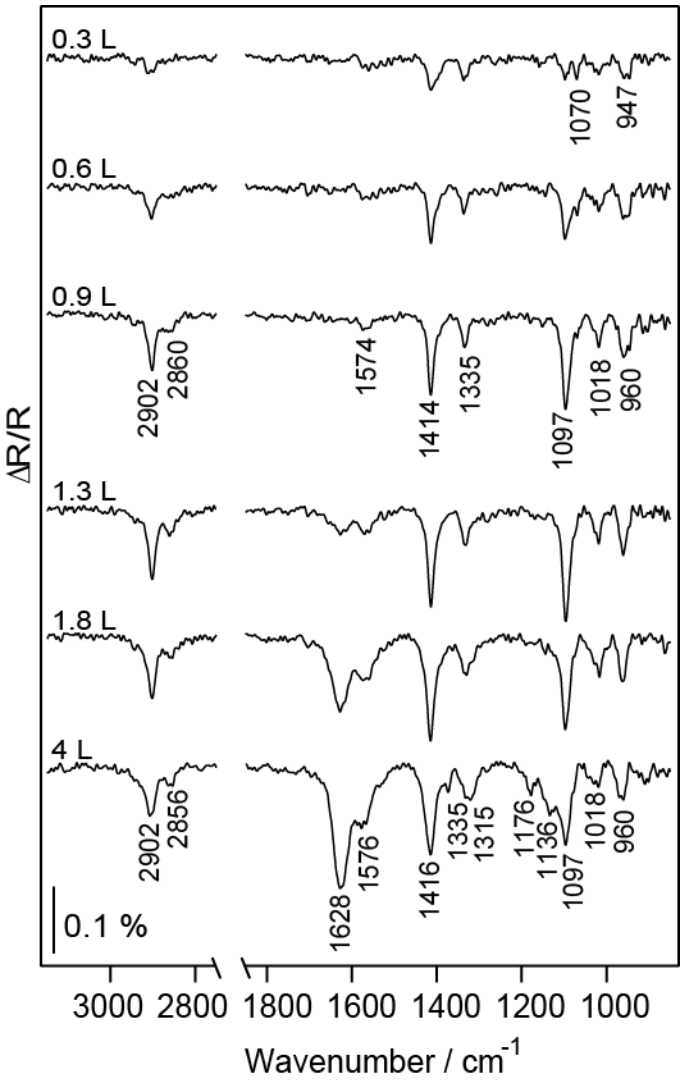

Figure 3: RAIR spectra obtained with increasing exposures of glycine at 3×10^{-9} mbar and 300 K.

Whether the amine group is protonated is more difficult to evaluate. Our RAIR spectra exhibit inconsistency in the infrared baseline above 3000 cm^{-1} (due to ice accumulation in the liquid nitrogen-cooled detector); the apparent absence of amine stretching modes (in the region $3250 - 3450$ cm^{-1}) after dosing glycine at 300 K may be a consequence of this, or of the nature and orientation of the adsorbed species. As a vibrational mode will only absorb infrared radiation if its dynamic dipole moment has a non-zero component perpendicular

to the surface,[34] the amine stretching modes would not be expected to have measurable intensity if the plane defined by the nitrogen and hydrogen atoms of the unprotonated amine group is close to parallel to the surface. In the RAIR spectra reported after dosing glycine on Cu{110} at 300 K, the amine stretching modes are similarly not present;[4] here, nitrogen 1s X-ray photoelectron spectroscopy has suggested that the amine group remains unprotonated,[6] and this conclusion has been supported by near-edge X-ray absorption fine structure, X-ray emission spectroscopy and photoelectron diffraction data.[5–7] Given the significant similarity between the RAIR spectra on the two surfaces, adsorption on Cu{311} in the anionic glycinate form appears most likely.

Figure 4 shows the LEED patterns observed from the clean Cu{311} surface, and with glycine exposures of 1 and 4 L at 300 K. At low exposures, additional sharp spots develop, indicating the presence of an ordered overlayer (the precise nature of which will be discussed subsequently); above 1 L, the spots become streaked. The development of both the LEED pattern and the RAIR spectrum therefore indicate that the monolayer that forms on dosing glycine onto Cu{311} at this temperature exhibits two distinct phases: a low-coverage phase is observed at exposures below around 1 L, with a high-coverage phase apparent at higher doses.

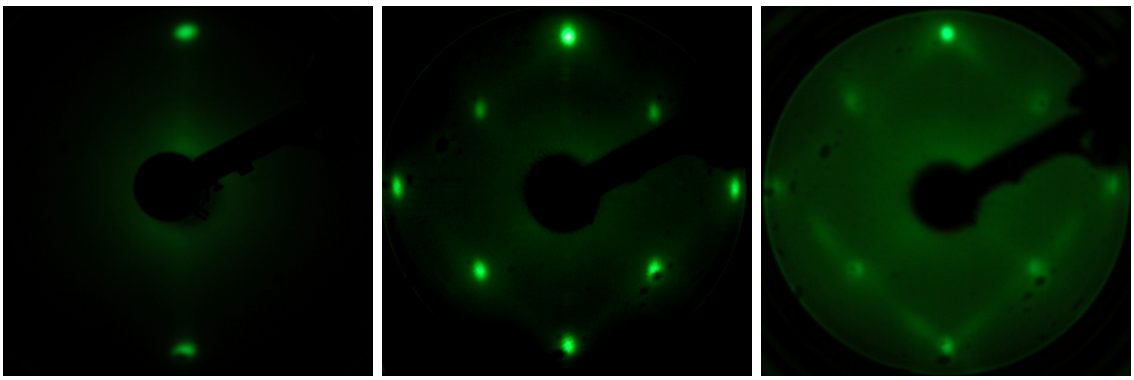

(a) clean surface (b) 1 L (c) 4 L

Figure 4: LEED patterns obtained at 19 eV from the clean Cu{311} surface, and at exposures of 1 and 4 L of glycine at 3×10^{-9} mbar and 300 K.

Low-coverage phase

We performed geometry optimisation calculations for isolated glycinate (within a $(3, 3; -1, 1)$ unit cell, a coverage of $\frac{1}{6}$ ML), using a range of starting geometries (Figure S-6 of the Supporting Information), in order to ascertain the most stable bonding configuration at very low coverages. Figure 5 shows three optimised geometries: (a), (b) and (c) are the lowest energy conformations for isolated three-point (μ3) bonded glycinate (in which the nitrogen atom and both oxygen atoms bond to surface atoms), two-point (μ2) bonded glycinate (in which the nitrogen atom and only one oxygen atom bond to the surface), and carboxylate-bonded glycinate (in which both oxygen atoms bond to the surface, but the nitrogen atom does not), respectively. These were the three bonding configurations proposed for glycinate on Cu{110} by Barlow et al.[4] μ3-bonded glycinate is calculated to be most stable, with μ2- and carboxylate-bonded glycinate less stable by 209 and 627 meV respectively.

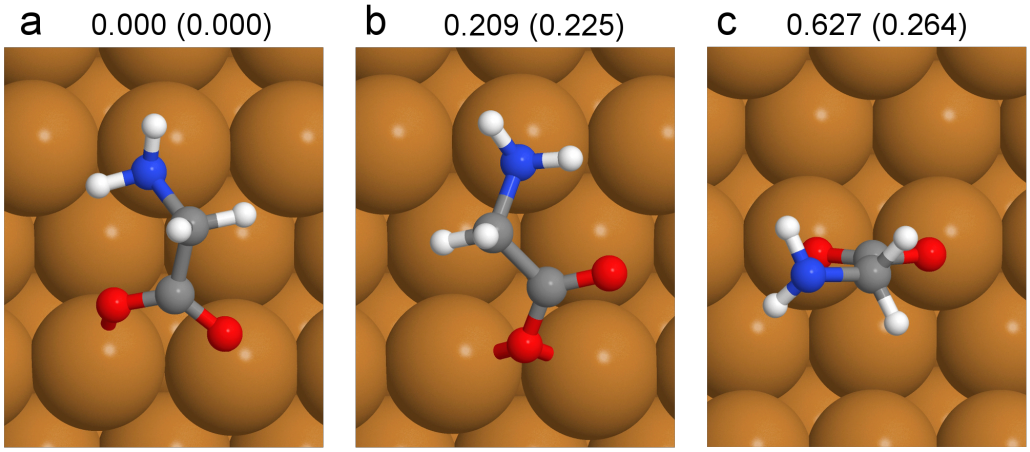

Figure 5: The lowest-energy geometries calculated for isolated (a) μ3-bonded, (b) μ2-bonded and (c) carboxylate-bonded glycinate (in $(3, 3; -1, 1)$ unit cells). The numbers give the energy difference (in eV) relative to the lowest-energy structure, with those in brackets not including van der Waals contributions.

Compared to the clean-surface LEED pattern (Figure 4 (a)), the low-coverage pattern (Figure 4 (b)) shows additional sharp spots. Due to the low beam energy at which the LEED patterns must be obtained, few spots can be observed: Figure 6 illustrates the diffraction pattern schematically, with the basis vectors defining the reciprocal-space unit cells of the

clean surface, $\mathbf{a}_1$* and $\mathbf{a}_2$*, and of the surface after dosing 1 L glycine, $\mathbf{b}_1$* and $\mathbf{b}_2$*, shown. By inspection of Figure 6, it is evident that $\mathbf{b}_1^* = \frac{1}{3}(2\mathbf{a}_1^* - \mathbf{a}_2^*)$ and $\mathbf{b}_2^* = \frac{1}{3}(-\mathbf{a}_1^* + 2\mathbf{a}_2^*)$. The reciprocal-space unit cell of the surface can therefore be described by the matrix $(\frac{2}{3}, -\frac{1}{3}; -\frac{1}{3}, \frac{2}{3})$; the matrix describing the real-space overlayer arrangement (the inverse transpose of the reciprocal-space matrix) is $(2, 1; 1, 2)$, indicating a repeat unit containing three outer-level surface atoms. Identical overlayer arrangements are also observed on Cu{311} at low exposures of L-alanine[2,24] and racemic alanine[25].

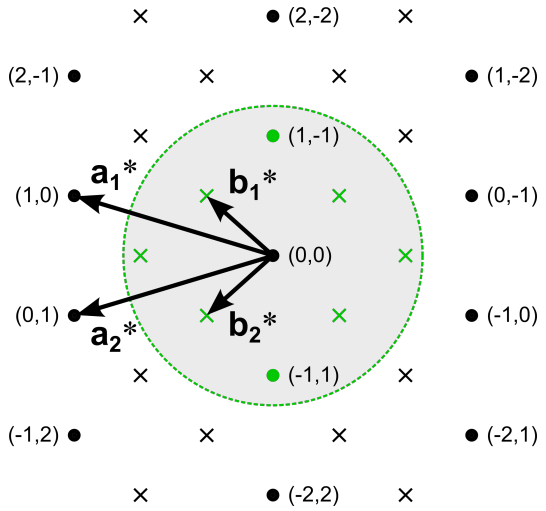

Figure 6: The spots present in the LEED patterns from the clean surface (dots) and after dosing 1 L glycine (crosses). The spots that can be seen on the screen at a beam energy of 19 eV are indicated in green. The basis vectors defining the reciprocal-space unit cells of the clean surface, $\mathbf{a}_1$* and $\mathbf{a}_2$*, and of the low-coverage phase, $\mathbf{b}_1$* and $\mathbf{b}_2$*, are marked, as are the indices of the integer-order spots.

We therefore also performed geometry optimisation calculations for glycinate within a $(2, 1; 1, 2)$ unit cell (a coverage of $\frac{1}{3}$ ML), using a range of starting geometries (Figure S-7 of the Supporting Information). Figure 7 shows three optimised geometries: (a), (b) and (c) are the lowest energy conformations in $(2, 1; 1, 2)$ arrangements for μ3-, μ2-, and carboxylate-bonded glycinate respectively. μ3-bonded glycinate is again calculated to be most stable, with $(2, 1; 1, 2)$ μ2- and carboxylate-bonded glycinate less stable by 167 and 834 meV respectively. Using the lowest-energy $(2, 1; 1, 2)$ structure (shown in Figure 7 (a)), we calculated vibrational frequencies for μ3-bonded glycinate; these are shown in Table 1, in addition to mode assignments

made by visual inspection of the calculated vibrations, and the frequencies of the absorptions present in the experimental low-exposure RAIR spectra. Comparison with the calculated frequencies allows assignment of the absorptions in the experimental data.

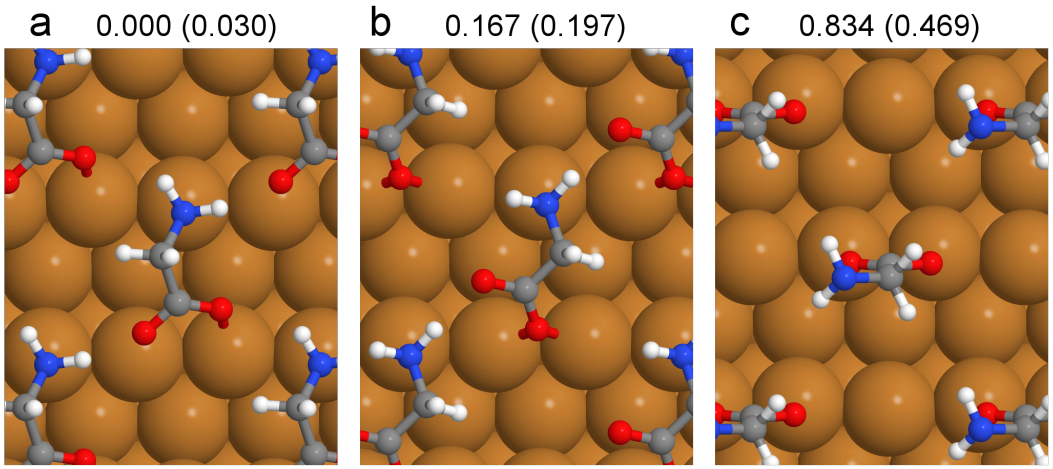

Figure 7: The lowest-energy geometries calculated for (a) μ3-bonded, (b) μ2-bonded and (c) carboxylate-bonded glycinate in $(2,1;1,2)$ unit cells. The numbers give the energy difference (in eV) relative to the lowest-energy structure, with those in brackets not including van der Waals contributions (in which case, the lowest-energy μ3-bonded geometry changes - see Figure S-7 of the Supporting Information).

The development of intense peaks at 1414 and 1097 cm^{-1} characterises the low-exposure RAIR spectra. The absorption at 1414 cm^{-1} corresponds to the vibration calculated for μ3-bonded glycinate at 1421 cm^{-1}, most closely resembling the scissoring deformation of the methylene group, $\delta_s(CH_2)$, and symmetric stretching of the carboxylate group, $\nu_s(CO_2)$. The presence of this absorption is consistent with the glycinate adopting a conformation similar to the calculated structure: both of the contributing modes have non-zero components perpendicular to the surface as long as the principal axes of the two groups are not parallel to the surface. The absorption at 1097 cm^{-1} corresponds to the vibration calculated at 1093 cm^{-1}, resembling wagging of the amine group, $\omega(NH_2)$, which has a large component of its dynamic dipole moment perpendicular to the surface, and a bending mode of the upper methylene hydrogen atom, $\delta(CH_{up})$, which is largely parallel to the surface.

Four additional peaks develop at 2902, 1335, 1018 and 960 cm^{-1}. These are assigned re-

Table 1: The calculated vibrational frequencies and corresponding mode assignments of μ3-bonded glycinate in a $(2,1;1,2)$ arrangement, and of isolated μ2-bonded glycinate, and frequencies of the absorptions present in the experimental low and high-exposure RAIR spectra. Additional calculated vibrational modes that lie outside the region where infrared absorptions can be detected in our experimental apparatus (the baseline is unstable at frequencies below 900 cm^{-1}) are not included.

calculated frequency / cm^{-1}		assignment	experimental frequency / cm^{-1}	
μ3	μ2		0.9 L	4 L
3399	3446	$\nu_a(NH_2)$		
3296	3346	$\nu_s(NH_2)$		
2965	2941	$\nu_a(CH_2)$	2902	2902
2834	2822	$\nu_s(CH_2)$	2860	2856
	1668	ν(C=O)		1628
1581		$\nu_a(CO_2) + \delta_s(NH_2)$	1574	1576
1529		$\delta_s(NH_2) + \nu_a(CO_2)$		
	1520	$\delta_s(NH_2)$		
	1446	$\delta_s(CH_2)$		
1421		$\delta_s(CH_2) + \nu_s(CO_2)$ [$+ \nu$(CC) $+ \tau(NH_2)$]	1414	1416
1395		$\nu_s(CO_2) + \delta_s(CH_2)$ [$+ \nu$(CC) $+ \tau(NH_2)$]		
	1376	ν(CC) $+ \omega(CH_2)$ [$+ \nu_s(CO_2) + \tau(NH_2)$]		
1331		$\omega(CH_2) + \nu_s(CO_2) + \tau(NH_2)$	1335	1335
				1315
	1275	ν(C−O) $+ \delta(CH_{up})$ [$+ \tau(NH_2)$]		
1273	1241	$\tau(CH_2) + \tau(NH_2)$		
				1176
1161	1140	$\tau(NH_2) + \delta(CH_{down})$		
				1136
1093	1083	$\omega(NH_2) + \tau(CH_2)$	1097	1097
1031	1015	ν(CN)	1018	1018
943	946	ω(CCN) [$+ \rho(CH_2) + \omega(NH_2)$]	960	960

spectively to antisymmetric stretching of the methylene group, $\nu_a(CH_2)$; to a combination of wagging of the methylene group, $\omega(CH_2)$, symmetric stretching of the carboxylate group and twisting of the amine group, $\tau(NH_2)$; to stretching of the C−N bond, $\nu(CN)$; and to a wagging-like deformation of the C−C−N backbone, $\omega(CCN)$.

Two weak absorptions are observed in the low-coverage phase, at 2860 and 1574 cm^{-1}. The peak at 2860 cm^{-1} is assigned to the symmetric stretching vibration of the methylene group, $\nu_s(CH_2)$, calculated at 2834 cm^{-1}. That this absorption is much less intense than that due to the analogous antisymmetric stretch may provide support for the principal axis of the methylene group being close to parallel to the surface. The peak at 1574 cm^{-1}corresponds to the vibration calculated at 1581 cm^{-1}, resembling antisymmetric stretching of the carboxylate group, $\nu_a(CO_2)$, and scissoring of the amine group, $\delta_s(NH_2)$. The weakness of this absorption, and the absence of any absorption due to the visually similar vibration calculated at 1529 cm^{-1}, are as expected for glycinate adopting μ3 bonding configurations, in which the two oxygen atoms are approximately equidistant from the surface, and consequently the dynamic dipole moment of the carboxylate antisymmetric stretching mode is parallel to the surface, as is the dynamic dipole moment of the amine scissoring deformation.

In addition to the amine stretching modes (calculated for μ3-bonded glycinate at 3399 and 3269 cm^{-1}) discussed previously, three further vibrations calculated between 3400 and 900 cm^{-1} are not observed in the low-exposure experimental spectra. The vibrations calculated at 1273 and 1161 cm^{-1} resemble twisting of the amine group, combined with twisting of the methylene group, $\tau(CH_2)$, and bending of the lower methylene hydrogen atom, $\delta(CH_{down})$, respectively. Neither of these vibrations has a significant component of its dynamic dipole moment perpendicular to the surface, so their absence from the experimental spectra is consistent with the glycinate adopting the conformation shown in Figure 7 (a). By contrast, the peak calculated at 1395 cm^{-1} is visually similar to that calculated at 1421 cm^{-1}; in both cases scissoring of the methylene group and symmetric stretching of the carboxylate group are expected to have non-zero components perpendicular to the surface. The most plausible

explanation for the absence of a clear peak at around 1395 cm^{-1} is that this is hidden by the large peak at 1414 cm^{-1}; the small shoulder at around 1400 cm^{-1}, which is most apparent at low exposures, may correspond to the vibration calculated at 1395 cm^{-1}.

High-coverage phase

At glycine exposures above 1 L at a Cu{311} surface temperature of 300 K, the LEED pattern becomes streaked in two mirror-image directions, as seen in Figure 4 (c). Simultaneously, an intense absorption develops in the RAIR spectra at 1628 cm^{-1}; no peak is seen close to this frequency in the low-coverage phase, or in the calculations of μ3-bonded glycinate in a $(2,1;1,2)$ arrangement. Species are now adopting a different bonding configuration: based on the energies of the calculated structures shown in Figures 5 and 7, a μ2 bonding configuration (in which one oxygen atom remains detached from the surface) is most likely.

To assign the peaks that develop in the high-exposure RAIR spectra, we have calculated the vibrational frequencies of isolated μ2-bonded glycinate in the calculated lowest-energy conformation (shown in Figure 5 (b)). Isolated species were considered in order to avoid unjustified assumptions about unknown nearest-neighbour configurations and interactions; unlike in the low-coverage phase, the streaked LEED pattern suggests that the overlayer lacks long-range order, and STM data indicate that the adsorbed species are likely to experience different local environments.[25] The presence of adjacent species will undoubtedly alter the precise conformation of the glycinate moiety: Whereas in our calculated structures, the carboxylate oxygen atom bonds to a bridge site, an atop position (which allows the μ2-bonded moiety to occupy only two surface atoms) appears more likely in the high-coverage overlayer. In addition, our calculations for isolated species neglect the contribution of intermolecular hydrogen bonding. However, the development of the RAIR spectrum in the high-coverage phase is very similar to that previously reported with glycine and alanine on Cu{110},[3,4] and with alanine on Cu{311};[24] in all three cases, this development was assigned to the presence

of μ2-bonded moieties. The similarity of the RAIR spectra therefore supports our use of a μ2 bonding configuration. Table 1 shows our calculated frequencies and the corresponding mode assignments, in addition to the frequencies of the absorptions in the experimental high-exposure RAIR spectra.

The absorption at 1628 cm^{-1} is assigned to the vibration calculated at 1668 cm^{-1}, resembling a stretching vibration of the carboxylate group in μ2-bonded glycinate. For glycinate on Cu{110}, a peak is present at high coverages at 1630 cm^{-1}; this has been assigned to anti-symmetric stretching of the carboxylate group in μ2-bonded species.[4] However, based on our theoretical calculations (and analogous to our previous calculations for μ2-bonded alaninate on Cu{311})[24], it appears that the two C−O bonds exhibit significantly different lengths: that to the surface-bound oxygen atom is 1.31 Å, typical of a C−O single bond,[35] whereas that to the oxygen atom not bonded to the surface is 1.23 Å, closer to the value expected for a C=O double bond.[35] Furthermore, the vibration calculated at 1668 cm^{-1} appears to be localised on the C=O bond. This therefore suggests that, although the frequency differs significantly to the 1716 cm^{-1} at which the carbonyl stretch in neutral species is observed in multilayer spectra on Cu{311} (see SI), assignment of the absorption at 1628 cm^{-1} to a C=O stretching mode, ν(C=O), is most accurate.

The extent to which the RAIR spectrum changes at high exposures is dependent on the glycine dosing pressure (Figure S-3 of the Supporting Information): at higher pressure, the absorption due to the C=O stretching mode is more intense, suggesting that more μ2-bonded species are present in the overlayer. Figure 8 (c) shows the difference between the high-exposure RAIR spectrum obtained after dosing 16 L glycine at 1×10^{-8} mbar, 8 (b), and that at the upper limit of the low-coverage phase, 8 (a), emphasizing the changes that occur in the high-coverage phase. The absorptions already present at 1097, 1018 and 960 cm^{-1} (assigned respectively to wagging of the amine group and bending of the upper methylene hydrogen atom, to stretching of the C−N bond, and to a wagging-like deformation of the C−C−N backbone) broaden and decrease in maximum intensity, most markedly in the case of

the 1097 cm^{-1} peak, with additional sub-peaks seemingly developing at 1176 and 1136 cm^{-1}. The broadening and intensity decreases of the peaks can be attributed to a combination of factors: firstly, although visually very similar vibrations to those to which the original peaks were assigned (calculated for μ3-bonded glycinate at 1093, 1031 and 943 cm^{-1}) are also observed for μ2-bonded species, the frequencies differ slightly (calculated at 1083, 1015 and 946 cm^{-1} respectively); in addition, there may be a reduction in the number of μ3-bonded species present, if some of those previously adsorbed convert to μ2 bonding configurations in order to allow the total coverage to increase above $\frac{1}{3}$ ML; finally, some μ3-bonded species may now adopt a slightly different conformation (for example, a different orientation of the C−C−N backbone), which may also change their vibrational frequencies and/or reduce the component of the dynamic dipole moment of some vibrations perpendicular to the surface. It is also possible that the peaks that develop at 1176 and 1136 cm^{-1} contain contributions from the vibration resembling twisting of the amine group and bending of the lower methylene hydrogen atom parallel to the surface, calculated for isolated μ2-bonded species at 1140 cm^{-1}; however, as this mode's dynamic dipole moment is only expected to have a small component perpendicular to the surface, this seems unlikely.

Figure 8 (c) also shows a significant increase in infrared absorption at 1425 cm^{-1} in the high-coverage phase. Initially, it may appear likely that this peak corresponds to the vibration calculated for μ2-bonded glycinate at 1446 cm^{-1}, assigned as the scissoring deformation of the methylene group. However, with the principal axis of the methylene group tilted to be close to parallel to the surface, this vibration would be expected to have a very small component perpendicular to the surface. In addition, in work reported on Cu{110}, where the absorption frequencies generally match those on Cu{311} to within a few wavenumbers, a significant absorption develops at 1441 cm^{-1} at high coverages of glycinate.[4] The most plausible explanation for these observations is that the principal axis of the methylene group is closer to perpendicular to the surface in μ2-bonded glycinate on Cu{110} than on Cu{311}, and consequently the scissoring deformation of the methylene group is only observed on

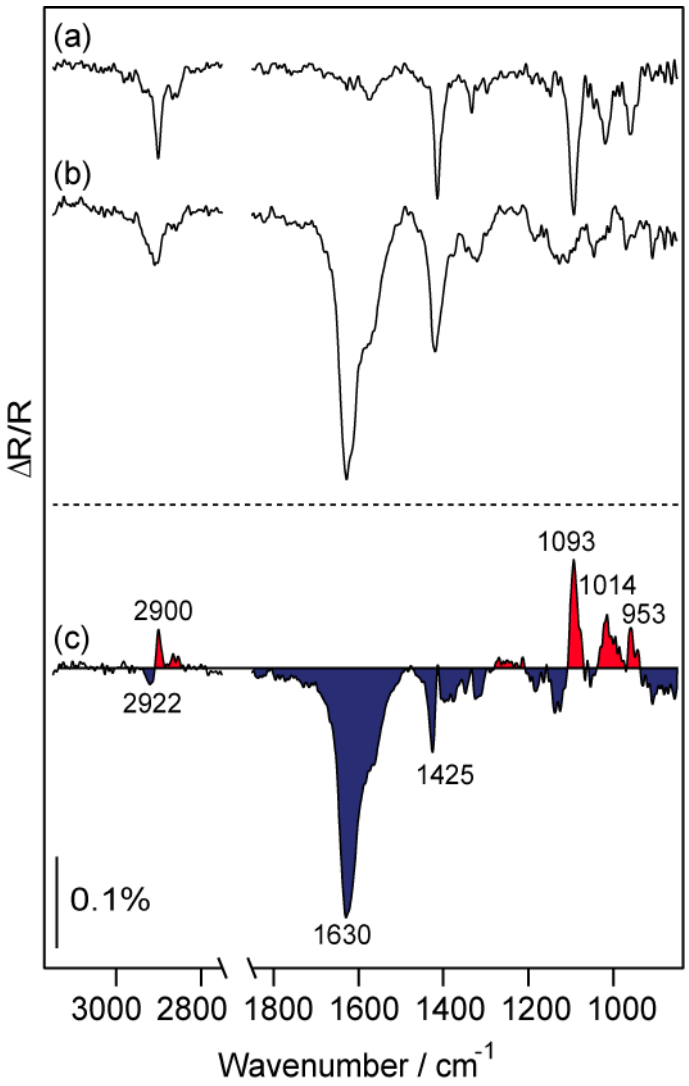

Figure 8: (a) and (b) RAIR spectra obtained after dosing (at 300 K) 1 L glycine at 3×10^{-9} mbar and 16 L glycine at 1×10^{-8} mbar respectively. (c) is the result of subtracting (a) from (b), emphasizing the changes to the spectrum in the high-coverage phase.

Cu{110}. The increase in absorption at 1425 cm^{-1} in the high-coverage phase on Cu{311} may result from a small broadening in the peak seen at 1414 cm^{-1} in the low-coverage phase, due to a reorientation of some of the μ3-bonded species in the increasingly crowded overlayer.

Figure 8 (c) shows an increase in infrared absorption in the high-coverage phase at 2922 cm^{-1}, and a decrease at 2900 cm^{-1}. Clearly these changes relate to the antisymmetric and symmetric stretching modes of the methylene group, calculated at 2965 and 2834 cm^{-1} respectively for μ3-bonded glycinate, and at 2941 and 2822 cm^{-1} respectively for isolated μ2-bonded species.

Given the comparatively poor agreement to these calculated frequencies, it is not possible to be certain whether the broadening of the previously sharp peak centred at 2902 cm^{-1} is a result of the μ2-bonded species that are now present, or of an increase in the heterogeneity of the orientations of the μ3-bonded species in the overlayer, or of a combination of these factors.

Additional small increases in infrared absorption in the high-coverage phase can be observed in the $1310 - 1405$ cm^{-1} region: There appears to be a broad increase between 1370 cm^{-1} and 1405 cm^{-1}, which may be associated with the vibrations calculated at 1395 cm^{-1} for μ3-bonded glycinate (resembling symmetric stretching of the carboxylate group and the scissoring deformation of the methylene group) and at 1376 $cm^{-1}$for μ2-bonded glycinate (resembling stretching of the C−C bond and wagging of the methylene group); although the former vibration did not result in a significant absorption at low coverages, a reorientation of the previously adsorbed μ3-bonded species would be consistent with this development in the high-coverage phase. Small increases between 1310 and 1350 cm^{-1} are due to a broadening of the low-coverage phase peak centred at 1335 cm^{-1}, which also indicates an increase in the heterogeneity of the orientations of the μ3-bonded species present in the overlayer.

Several of the vibrational modes calculated for μ2-bonded glycinate are not observed in the experimental RAIR spectra. The stretching modes of the amine group (calculated at 3446 and 3346 cm^{-1}) are not present, as discussed previously. The absence of absorptions due to the scissoring deformations of the amine and methylene groups (calculated at 1520 and 1446 cm^{-1} respectively) are likely to be a consequence of the principal axes of the two groups, and hence the dynamic dipole moments of the two vibrations, being close to parallel to the surface. As in the low-coverage phase, the vibrations resembling twisting of the amine group combined with twisting of the methylene group and bending of the lower methylene hydrogen atom, calculated at 1241 and 1140 cm^{-1} respectively, are not expected to be RAIRS active. However, the fact that no absorption is observed around 1275 cm^{-1} in the high-coverage phase is somewhat surprising: the vibration calculated at that frequency resembles stretching of the

C−O bond to the surface-bound oxygen atom (in addition to bending of the upper methylene hydrogen atom). In the calculated μ2-bonded geometry, the dynamic dipole moment of this vibration would be expected to have a significant component perpendicular to the surface. The absence of this peak may therefore indicate that the C−O bond lies closer to parallel to the surface than in the geometry calculated for isolated μ2-bonded glycinate: this would be due to the interactions (including both repulsive steric interactions and attractive hydrogen bonding) between adjacent species in the overlayer.

Figure 9 shows RAIR spectra obtained after progressively annealing a high-coverage overlayer at increasing temperatures. At temperatures as low as 350 K, the 1628 cm^{-1} peak is observed to have started decreasing in intensity, disappearing completely at 460 K. Reversion of the previously discussed peaks at the low-wavenumber end of the spectrum is also observed from 350 K, with the peaks assigned to μ3-bonded glycinate sharpening and increasing in intensity. This development is the reverse of what is observed on dosing glycine at 300 K, at exposures above 1 L. Similarly, LEED (Figure S-5 of the Supporting Information) also indicates progressive reversion to the low-coverage phase by 460 K, with the streaking having disappeared, and the pattern reverting to that indicating a $(2,1;1,2)$ overlayer arrangement. On annealing above 460 K, the remaining RAIRS peaks decrease in intensity and the non-integer spots in the LEED pattern fade. At 480 K, neither RAIRS nor LEED show any evidence of adsorbed species remaining on the surface.

Glycine and alanine on Cu{311} and Cu{110}

In their work on Cu{110}, Barlow et al.[4] assigned RAIRS absorptions to vibrations of specific functional groups of glycinate by reference to previous infrared studies of different forms of glycine; our calculation-based assignments reflect the fact that the vibrations involve the whole species, rather than being localised on a single functional group. However, in most cases there is very good agreement between both the absorption frequencies and the

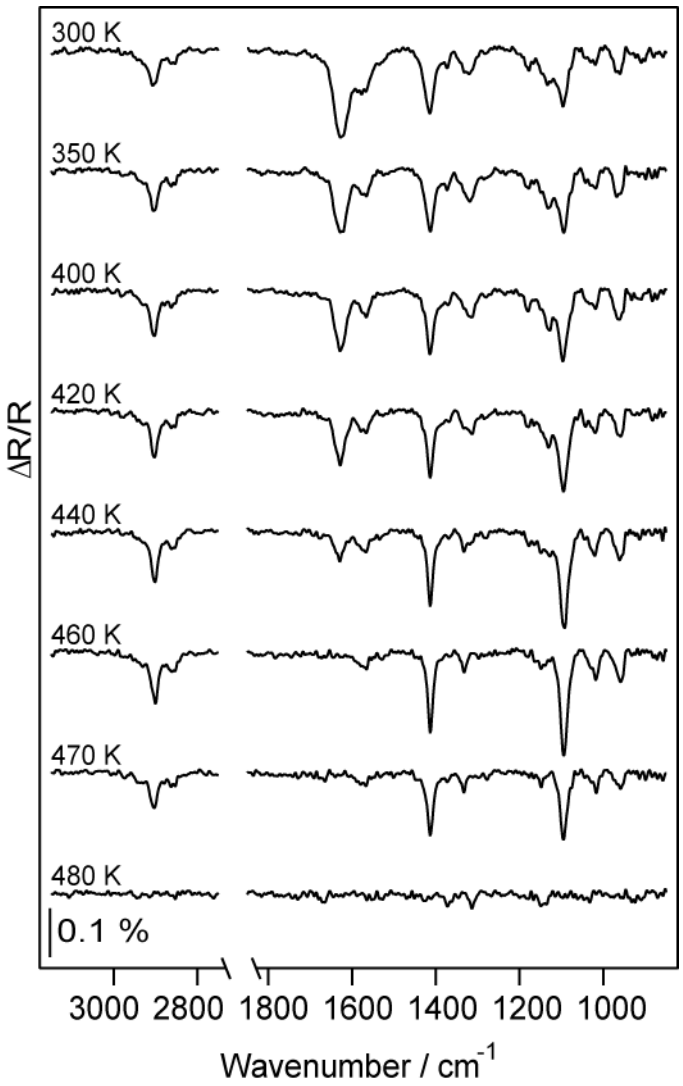

Figure 9: RAIR spectra obtained after dosing 4 L glycine at 3×10^{-9} mbar and 300 K, and after subsequently heating the crystal at 1 Ks^{-1} up to the specified temperature, annealing for two minutes, then cooling back to 300 K.

assignments on the two surfaces, as shown in Table 2. The only exception regards the absorption observed at 960 cm^{-1} on Cu{311}, which we have assigned to a wagging-like deformation of the C−C−N backbone (calculated at 943 and 946 cm^{-1} for μ3- and μ2-bonded glycinate respectively). Two separate peaks are reported on Cu{110}, at 969 and 945 cm^{-1} at low coverages, and at 985 and 902 cm^{-1} at high coverages. These are assigned respectively to stretching of the C−C bond, and rocking of the methylene group. It is noteworthy that on Cu{311} at very low exposures, an absorption at 947 cm^{-1} can be distinguished

from that at 960 cm^{-1}. However, as the two peaks do not develop in the same manner with increasing coverage, it appears probable that they are due to species adopting slightly different conformations, as opposed to different vibrational modes of the same species.

Table 2: A comparison of the frequencies of the absorptions present in the RAIR spectra after low and high glycine exposures, and the corresponding mode assignments, on Cu{110} [4] and Cu{311}.

Cu{110}			Cu{311}		
frequency / cm^{-1}		assignment	frequency / cm^{-1}		assignment
low	high		0.9 L	4 L	
2906	2910	$\nu_a(CH_2)$	2902	2902	$\nu_a(CH_2)$
2860	2860	$\nu_s(CH_2)$	2860	2856	$\nu_s(CH_2)$
	1630	$\nu_a(CO_2)$		1628	ν(C=O)
	1578	$\delta_s(NH_2)$	1574	1576	$\nu_a(CO_2) + \delta_s(NH_2)$
	1441	$\delta_s(CH_2)$			$\delta_s(CH_2)$
1417	1422	$\nu_s(CO_2)$	1414	1416	$\delta_s(CH_2) + \nu_s(CO_2)$ [$+ \nu$(CC) $+ \tau(NH_2)$]
1332	1320	$\omega(CH_2)$	1335	1335	$\omega(CH_2) + \nu_s(CO_2) + \tau(NH_2)$
1088	1105	$\omega(NH_2)$	1097	1097	$\omega(NH_2) + \tau(CH_2)$
1024		ν(CN)	1018	1018	ν(CN)
969	985	ν(CC)	960	960	ω(CCN) [$+ \rho(CH_2) + \omega(NH_2)$]
945	902	$\rho(CH_2)$			

The significant similarity between the RAIR spectra obtained with increasing exposures of glycine on Cu{311} and Cu{110} suggests that the adsorbing glycinate moieties adopt similar bonding configurations on the two surfaces. Our theoretical calculations indicate that the energy of a glycinate moiety bonding to the Cu{311} surface through its carboxylate group only (with the amine group directed away from the surface, as proposed previously at low coverages on Cu{110}) [4] would be prohibitively high: μ3 bonding at low coverages therefore appears most probable.

The behaviour indicated by the RAIR spectra obtained with increasing exposures of glycine on Cu{311} and Cu{110} at room temperature is very similar to that indicated by analogous spectra with enantiopure L-alanine[24] and racemic alanine (Figure S-4 of the Supporting

Information) on Cu{311}, and also with the same molecules on Cu{110}[3,19]: in all cases, the carboxylic acid groups of the molecules deprotonate on adsorption and the resulting anionic species most likely adopt only μ3 bonding configurations at low exposures, with μ3- and μ2-bonded species coexisting at high exposures. Despite the species adopting the same bonding configurations, the nature of the ordered arrangements formed and the behaviour observed on annealing high glycinate or alaninate coverages differ significantly on the two surfaces.

In the low-coverage (μ3-only) phase on Cu{311}, the alaninate or glycinate moieties form well-ordered achiral $(2,1;1,2)$ arrangements at room temperature.[24,25] These low-coverage arrangements also form on annealing a high coverage at around 440 K. Although one group has reported the formation of a poorly-ordered (3×2) overlayer on dosing glycine at room temperature on Cu{110} (with a LEED pattern that sharpens on annealing at 413 K),[4] no hint of an ordered arrangement is observed on dosing alanine at room temperature. Ordered (3×2) arrangements have only been reported on Cu{110} on annealing high coverages of racemic and enantiopure alaninate at above 358 K and 470 K respectively.[19]

This difference in behaviour can be viewed as a consequence of the existence of "footprint chirality" for μ3-bonded species on Cu{110}, and its absence on Cu{311}. Previous studies of α-amino acid adsorption on copper surfaces have used two different definitions of footprint for μ3-bonded species: (a) the triangle defined by the points of contact between the adsorbate and the surface[19] and (b) the triangle defined by the three surface atoms to which the molecule bonds[2]. In this study, we apply the latter definition, because it facilitates a simplified analysis based on the different registries of adjacent close-packed rows on the Cu{110} and Cu{311} surfaces. With that in mind, when the two carboxylate oxygen atoms bond to adjacent surface atoms in a close-packed row on Cu{110}, the amine nitrogen atom can bond to either of two surface atoms in the next close-packed row; the three copper atoms bonded to the glycinate or alaninate moiety define chiral right-angled triangular footprints (Figure 10).[19] When the two carboxylate oxygen atoms bond to adjacent surface atoms in a

close-packed row on Cu{311}, the amine nitrogen atom can only bond to one surface atom in the next close-packed row; the three copper atoms bonded to the glycinate or alaninate moiety define an achiral isosceles triangular footprint (Figure 10).[2]

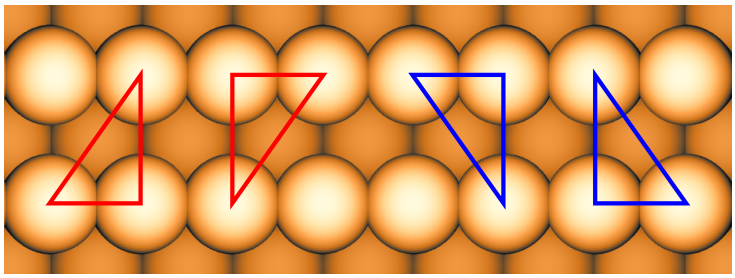

(a) Cu{110}

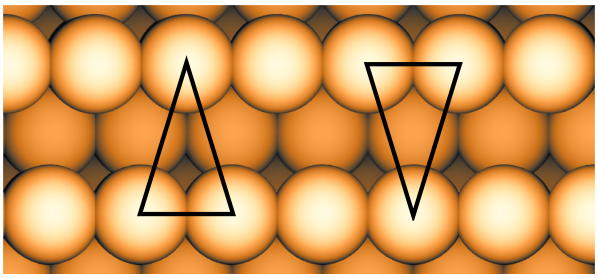

(b) Cu{311}

Figure 10: The possible μ3 bonding configurations for a simple amino acid on (a) Cu{110} and (b) Cu{311}. In (a), the red footprints (which are equivalent to each other) have an enantiomeric relationship with the blue footprints (also equivalent to each other), and so the system exhibits footprint chirality. In (b), as the footprints possess mirror symmetry, the system does not exhibit footprint chirality. The two bonding configurations are energetically inequivalent: for isolated glycinate, the left hand footprint is calculated to be favoured by 0.047 eV (see Figure S-6 of the Supporting Information).

For the (3×2) structure to form on Cu{110}, the two μ3-bonded species in the unit cell must adopt mirror-image ("heterochiral") footprints (Figure S-8 of the Supporting Information). For isolated glycinate, the two mirror-image footprints are energetically equivalent; the same is not true for alaninate, as the presence of the methyl group makes the two backbone distortions inequivalent, with L- and D-alaninate favouring mirror-image footprints.[16] The high temperature annealing required to form the ordered (3×2) alaninate arrangements may be a consequence of the energy barrier that must be overcome to allow the alaninate moieties to adopt heterochiral footprints. By contrast, L- and D-alaninate and glycinate are

all expected to favour the same μ3 footprint on Cu{311}, which allows a (2,1;1,2) arrangement to form readily at room temperature in all three cases.

In the high-coverage (μ3 and μ2) phase on Cu{311}, the $(2,1;1,2)$ LEED pattern becomes streaked and STM images show chirally oriented rows of features: with enantiopure alanine, the streaking breaks the symmetry of the clean-surface pattern and the chiral "boundaries" run in one direction;[24] with racemic alanine and glycine, the streaking is symmetric and the boundaries are in two mirror-image directions.[25] It should be noted that it is possible for alaninate and glycinate to adopt chiral μ2 footprints (with respect to the underlying surface symmetry) on both Cu{110}[15] and Cu{311}[24]. Whereas chirality in the high-coverage alaninate overlayers may be a manifestation of the molecular chirality of the adsorbed species, in the case of glycine on Cu{311}, the mirror-image boundaries must be a consequence of asymmetry generated on adsorption of the μ2-bonded species. By contrast, both chiral and achiral μ2 footprints are possible on Cu{110}: the disorder in the high-coverage glycinate overlayer (reported in LEED experiments)[4] may be a consequence of the adsorbed species adopting up to five different footprints.

Conclusions

A combination of RAIRS, LEED and DFT calculations have been used to investigate the bonding, conformation and self-assembly of glycine on Cu{311}. Our RAIRS and DFT results confirm that, similarly to what is observed on Cu{110}, glycinate can adopt both three-point (μ3) and two-point (μ2) footprints on Cu{311}, with the nitrogen atom occupying an atop site on a close-packed row and one or two oxygen atoms of the carboxylic acid group bonding to copper atoms in an adjacent row. At low coverages, LEED experiments indicate that the μ3-bonded glycinate moieties form an achiral $(2,1;1,2)$ arrangement at room temperature. This is a consequence of the glycinate species adopting the isosceles μ3 footprint possible on the Cu{311} surface; in contrast, the different registry of close-packed

rows means that two chiral right-angled μ3 footprints are possible on Cu{110}. High-coverage RAIR spectra show the coexistence of μ3- and μ2-bonded glycinate, with some previously μ3-bonded species changing molecular conformation. Simultaneous development of streaking in the LEED pattern indicates restructuring of the self-assembled overlayer and disorder in two mirror-image directions. This is consistent with the formation of a racemic mixture of chiral boundaries between $(2,1;1,2)$ domains: the lack of molecular chirality and μ3 footprint chirality suggests that chirality in the high-coverage overlayer must be a consequence of the presence of μ2-bonded species. The present work has therefore helped to elucidate the subtle interplay between molecular and footprint chirality on the breaking of symmetry at surfaces; further work is in progress to determine the precise adsorbate conformations in the chiral overlayers.

Supporting Information

TPD data obtained after dosing glycine at 300 K; RAIR spectra obtained after dosing glycine at 100 K, after dosing glycine at different pressures at 300 K, and whilst dosing racemic alanine at 300 K; LEED patterns obtained after dosing glycine at 300 K and annealing at higher temperatures; all optimised geometries calculated for glycinate within $(3,3;-1,1)$ and $(2,1;1,2)$ unit cells; a schematic diagram of a (3×2) arrangement of μ3-bonded amino acid species adopting heterochiral footprints on Cu{110}. This material is available free of charge via the Internet at http://pubs.acs.org.

Acknowledgments

We acknowledge financial support from the Engineering and Physical Sciences Research Council.

References

(1) Ernst, K. H. Molecular Chirality at Surfaces. *Phys. Status Solidi B* **2012**, *249*, 2057–2088.

(2) Clegg, M. L.; Morales de la Garza, L.; Karakatsani, S.; King, D. A.; Driver, S. M. Chirality in Amino Acid Overlayers on Cu Surfaces. *Top. Catal.* **2011**, *54*, 1429–1444.

(3) Williams, J.; Haq, S.; Raval, R. The Bonding and Orientation of the Amino Acid L-Alanine on Cu{110} Determined by RAIRS. *Surf. Sci.* **1996**, *368*, 303–309.

(4) Barlow, S. M.; Kitching, K. J.; Haq, S.; Richardson, N. V. A Study of Glycine Adsorption on a Cu{110} Surface Using Reflection Absorption Infrared Spectroscopy. *Surf. Sci.* **1998**, *401*, 322–335.

(5) Booth, N. A.; Woodruff, D. P.; Schaff, O.; Giessel, T.; Lindsay, R.; Baumgartel, P.; Bradshaw, A. M. Determination of the Local Structure of Glycine Adsorbed on Cu(110). *Surf. Sci.* **1998**, *397*, 258–269.

(6) Hasselstrom, J.; Karis, O.; Weinelt, M.; Wassdahl, N.; Nilsson, A.; Nyberg, M.; Pettersson, L. G. M.; Samant, M. G.; Stohr, J. The Adsorption Structure of Glycine Adsorbed on Cu(110); Comparison with Formate and Acetate/Cu(110). *Surf. Sci.* **1998**, *407*, 221–236.

(7) Hasselstrom, J.; Karis, O.; Nyberg, M.; Pettersson, L. G. M.; Weinelt, M.; Wassdahl, N.; Nilsson, A. The Bonding and Electronic Structure Changes Upon Adsorption of Important Functional Groups: Glycine on Copper. *J. Phys. Chem. B* **2000**, *104*, 11480–11483.

(8) Nyberg, M.; Hasselstrom, J.; Karis, O.; Wassdahl, N.; Weinelt, M.; Nilsson, A.; Pettersson, L. G. M. The Electronic Structure and Surface Chemistry of Glycine Adsorbed on Cu(110). *J. Chem. Phys.* **2000**, *112*, 5420–5427.

(9) Chen, Q.; Frankel, D. J.; Richardson, N. V. Chemisorption Induced Chirality: Glycine on Cu{110}. *Surf. Sci.* **2002**, *497*, 37–46.

(10) Nyberg, M.; Odelius, M.; Nilsson, A.; Pettersson, L. G. M. Hydrogen Bonding between Adsorbed Deprotonated Glycine Molecules on Cu(110). *J. Chem. Phys.* **2003**, *119*, 12577–12585.

(11) Toomes, R. L.; Kang, J. H.; Woodruff, D. P.; Polcik, M.; Kittel, M.; Hoeft, J. T. Can Glycine Form Homochiral Structural Domains on Low-Index Copper Surfaces? *Surf. Sci.* **2003**, *522*, L9–L14.

(12) Kang, J. H.; Toomes, R. L.; Polcik, M.; Kittel, M.; Hoeft, J. T.; Efstathiou, V.; Woodruff, D. P.; Bradshaw, A. M. Structural Investigation of Glycine on Cu(100) and Comparison to Glycine on Cu(110). *J. Chem. Phys.* **2003**, *118*, 6059–6071.

(13) Barlow, S. M.; Louafi, S.; Le Roux, D.; Williams, J.; Muryn, C.; Haq, S.; Raval, R. Supramolecular Assembly of Strongly Chemisorbed Size- and Shape-Defined Chiral Clusters: S- and R-Alanine on Cu(110). *Langmuir* **2004**, *20*, 7171–7176.

(14) Rankin, R. B.; Sholl, D. S. Assessment of Heterochiral and Homochiral Glycine Adlayers on Cu(110) Using Density Functional Theory. *Surf. Sci.* **2004**, *548*, 301–308.

(15) Barlow, S. M.; Louafi, S.; Le Roux, D.; Williams, J.; Muryn, C.; Haq, S.; Raval, R. Polymorphism in Supramolecular Chiral Structures of R- and S-Alanine on Cu(110). *Surf. Sci.* **2005**, *590*, 243–263.

(16) Rankin, R. B.; Sholl, D. S. Structure of Enantiopure and Racemic Alanine Adlayers on Cu(110). *Surf. Sci.* **2005**, *574*, L1–L8.

(17) Rankin, R. B.; Sholl, D. S. Structures of Glycine, Enantiopure Alanine, and Racemic Alanine Adlayers on Cu(110) and Cu(100) Surfaces. *J. Phys. Chem. B* **2005**, *109*, 16764–16773.

(18) Jones, G.; Jones, L. B.; Thibault-Starzyk, F.; Seddon, E. A.; Raval, R.; Jenkins, S. J.; Held, G. The Local Adsorption Geometry and Electronic Structure of Alanine on Cu{110}. *Surf. Sci.* **2006**, *600*, 1924–1935.

(19) Haq, S.; Massey, A.; Moslemzadeh, N.; Robin, A.; Barlow, S. M.; Raval, R. Racemic Versus Enantiopure Alanine on Cu(110): An Experimental Study. *Langmuir* **2007**, *23*, 10694–10700.

(20) Unac, R. O.; Vidales, A. M.; Zgrablich, G. Effect of Interaction Energies on the Adsorption of Glycine onto a Cu(110) Surface: A Monte Carlo Simulation. *Adsorpt. Sci. Technol.* **2009**, *27*, 633–642.

(21) Zheleva, Z. V.; Eralp, T.; Held, G. Complete Experimental Structure Determination of the p(3x2)pg Phase of Glycine on Cu{110}. *J. Phys. Chem. C* **2012**, *116*, 618–625.

(22) Pratt, S. J.; Jenkins, S. J.; King, D. A. The Symmetry and Structure of Crystalline Surfaces. *Surf. Sci.* **2005**, *585*, L159–L165.

(23) Jenkins, S. J.; Pratt, S. J. Beyond the Surface Atlas: A Roadmap and Gazetteer for Surface Symmetry and Structure. *Surf. Sci. Rep.* **2007**, *62*, 373–429.

(24) Madden, D. C.; Temprano, I.; Sacchi, M.; Blanco-Rey, M.; Jenkins, S. J.; Driver, S. M. Self-Organized Overlayers Formed by Alanine on Cu{311} Surfaces. *J. Phys. Chem. C* **2014**, *118*, 18589–18603.

(25) Madden, D. C.; Bentley, M. L.; Jenkins, S. J.; Driver, S. M. On the Role of Molecular Chirality in Amino Acid Self-Organisation on Cu{311}. *Surf. Sci.* **2014**, *629*, 81–87.

(26) Segall, M. D.; Lindan, P. J. D.; Probert, M. J.; Pickard, C. J.; Hasnip, P. J.; Clark, S. J.; Payne, M. C. First-Principles Simulation: Ideas, Illustrations and the CASTEP Code. *J. Phys. Condens. Mat.* **2002**, *14*, 2717–2744.

(27) Clark, S. J.; Segall, M. D.; Pickard, C. J.; Hasnip, P. J.; Probert, M. J.; Refson, K.; Payne, M. C. First Principles Methods Using CASTEP. *Z. Kristallogr.* **2005**, *220*, 567–570.

(28) Perdew, J. P.; Burke, K.; Ernzerhof, M. Generalized Gradient Approximation Made Simple (vol 77, pg 3865, 1996). *Phys. Rev. Lett.* **1997**, *78*, 1396–1396.

(29) Monkhorst, H. J.; Pack, J. D. Special Points for Brillouin-Zone Integrations. *Phys. Rev. B* **1976**, *13*, 5188–5192.

(30) Vanderbilt, D. Soft Self-Consistent Pseudopotentials in a Generalized Eigenvalue Formalism. *Phys. Rev. B* **1990**, *41*, 7892–7895.

(31) Tkatchenko, A.; Scheffler, M. Accurate Molecular Van Der Waals Interactions from Ground-State Electron Density and Free-Atom Reference Data. *Phys. Rev. Lett.* **2009**, *102*, 073005 1–4.

(32) Refson, K.; Tulip, P. R.; Clark, S. J. Variational Density-Functional Perturbation Theory for Dielectrics and Lattice Dynamics. *Phys. Rev. B* **2006**, *73*, 155114 1–12.

(33) Halls, M. D.; Velkovski, J.; Schlegel, H. B. Harmonic Frequency Scaling Factors for Hartree-Fock, S-VWN, B-LYP, B3-LYP, B3-PW91 and MP2 with the Sadlej pVTZ Electric Property Basis Set. *Theor. Chem. Acc.* **2001**, *105*, 413–421.

(34) Hoffmann, F. M. Infrared Reflection-Absorption Spectroscopy of Adsorbed Molecules. *Surf. Sci. Rep.* **1983**, *3*, 109–192.

(35) Haynes, W. M. *Crc Handbook of Chemistry and Physics (95th Edition)*; CRC Press, 2014.

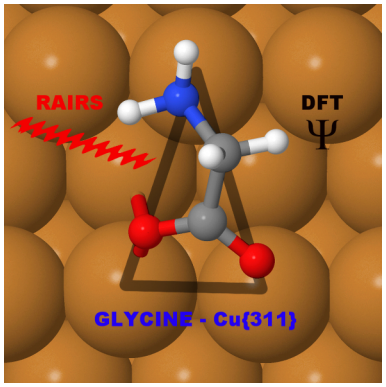

Figure 11: Table of Contents Image